Labeling Proteins with Fluorophore/Thioamide Förster Resonant Energy Transfer Pairs by Combining Unnatural Amino Acid Mutagenesis and Native Chemical Ligation

Rebecca F. Wissner, Solongo Batjargal, Colin M. Fadzen & E. James Petersson

Department of Chemistry, University of Pennsylvania
231 South 34th Street, Philadelphia, Pennsylvania 19104-6323 USA

General Information. A QuickChange® site-directed mutagenesis kit was purchased from Stratagene (La Jolla, CA). DNA oligomers were purchased from Integrated DNA Technologies, Inc (Coralville, IA). DNA sequencing was performed at the University of Pennsylvania DNA sequencing facility. Protein purification was conducted on a BioCad Sprint fast protein liquid chromatography (FPLC) system (GMI Inc.; Ramsey, MN; originally from Perseptive Biosystems). HPLC purification was carried out on a Varian Prostar system (currently Agilent Technologies; Santa Clara, CA). Intein plasmid pTXB1 and all restriction enzymes were purchased from New England Biolabs (Ipswich, MA).

Synthesis of Thiophenylalanine Precursor Compound.

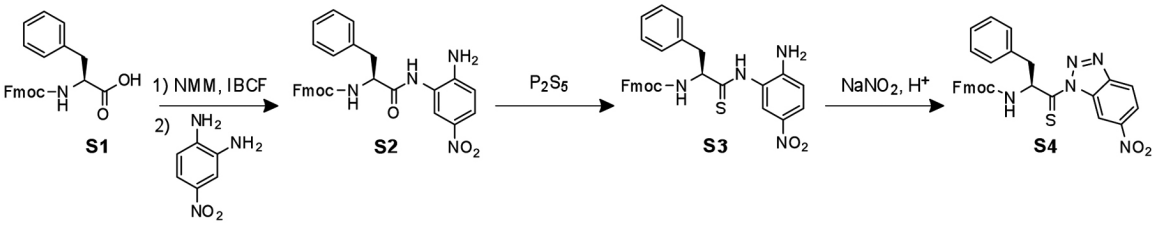

Scheme S1. Synthesis of thiophenylalanine nitrobenzotriazolide precursor.

Synthesis of the thiophenylalanine nitrobenzotriazolide precursor compound **S4** was based on a slight modification of the procedure originally reported by Shalaby *et al*.[1,2]

CaM Peptide Synthesis and Purification. Peptide synthesis was performed as described in the main text. CaM binding peptides were synthesized on Rink amide resin. Peptides were purified by reverse-phase HPLC using a binary system of aqueous (Buffer A: water + 0.1% TFA) and organic (Buffer B: CH_3CN + 0.1% TFA) phases. Solvent gradients, column descriptions, and retention times are listed in Tables **S1** and **S2**. Purified peptides were lyophilized or dried in a vacuum centrifuge.

Table S1. Summary of Purified Peptides.

Peptide	Gradient Description†	Retention Time (min)	Column (Size: Brand)
FRRIARLVGVLREFAFR (pOCNC)	S1	19.6	Semi-prep: Vydac 218 TP C18
F'RRIARLVGVLREFAFR (pOCNC-F′$_1$)	S1	20.6	Semi-prep: Vydac 218 TP C18
FRRIARLVGVL'REFAFR (pOCNC-L′$_{11}$)	S1	22.1	Semi-prep: Vydac 218 TP C18
FRRIARLVGVLREFAF'R‡ (pOCNC-F′$_{16}$)	S2	13.3, 14.2	Prep: Waters C18

†Described in Table S2. ‡Separable epimers were observed during HPLC purification.

Table S2. Solvent Gradients Used for Peptide Purification and Analysis.

Gradient	Time (min)	Buffer A (%)	Gradient	Time (min)	Buffer A (%)
S1	0:00	98	S2	0:00	98
	5:00	98		5:00	98
	8:00	71		9:00	69
	29:00	59		25:00	67
	33:00	0		27:00	0
	38:00	0		30:00	0
	43:00	98		35:00	98

Table S3. Calculated and Observed Peptide and Protein Masses.

Peptide	Calculated m/z $[M+H]^+$	Observed m/z $[M+H]^+$	Calculated m/z $[M+Na]^+$	Observed m/z $[M+Na]^+$
FRRIARLVGVLREFAFR (pOCNC)	2106.26	2106.75	2128.24	--
F'RRIARLVGVLREFAFR (pOCNC-F′$_1$)	2122.23	2122.43	2128.24	--
FRRIARLVGVL'REFAFR (pOCNC-L′$_{11}$)	2122.23	2122.16	2128.24	--
FRRIARLVGVLREFAF'R‡ (pOCNC-F′$_{16}$)	2122.23	2122.62	2128.24	--
CaM F*$_{13}$F$_{100}$F$_{139}$ (CaM^{F}F*$_{13}$)	16700.3	16699.8	16722.3	--
CaM F*$_{93}$F$_{100}$F$_{139}$ (CaM^{F}F*$_{93}$)	16700.3	16699.9	16722.3	--
CaM F*$_{100}$F$_{139}$ (CaM^{F}F*$_{100}$)	16700.3	16700.6	16722.3	--

Cloning of Calmodulin Expression Constructs. A plasmid containing the wild-type chicken calmodulin (CaM) gene was provided by Joshua Wand from the University of Pennsylvania School of Medicine. An insert containing the CaM gene was cloned into a pET15b vector (Novagen, Gibbstown, NJ) between the NcoI and XhoI cut sites. Quikchange® mutagenesis was used to generate the following mutant plasmids: pET15b-CaM-TAG$_{13}$F$_{100}$F$_{139}$, pET15b-CaM-TAG$_{17}$F$_{100}$F$_{139}$, pET15b-CaM-TAG$_{93}$F$_{100}$F$_{139}$, and pET15b-CaM-TAG$_{100}$F$_{139}$.

DNA Oligomers used for CaM Quikchange® Mutagenesis

a. Mutation F_{13} to TAG
Forward: 5' – ACTGACAGAAGAGCAGATTGCAGAATAGAAAGAAGCTTTTTCACTATTTGAC – 3'
Reverse: 5' – GTCAAATAGTGAAAAAGCTTCTTTCTATTCTGCAATCTGCTCTTCTGTCAGT – 3'

b. Mutation F_{17} to TAG
Forward: 5' – GATTGCAGAATTCAAAGAAGCTTAGTCACTATTTGACAAGGATGGT – 3'
Reverse: 5' – ACCATCCTTGTCAAATAGTGACTAAGCTTCTTTGAATTCTGCAATC – 3'

c. Mutation F_{93} to TAG
Forward: 5' – AATTAGAGAAGCGTTCCGTGTGTAGGACAAGGATGG – 3'
Reverse: 5' – CCATCCTTGTCCTACACACGGAACGCTTCTCTAATT – 3'

d. Mutation Y_{100} to F
Forward: 5' – GACAAGGATGGTAATGGTTTCATTAGTGCTGCAGAACTT – 3'
Reverse: 5' – AAGTTCTGCAGCACTAATGAAACCATTACCATCCTTGTC – 3'

d. Mutation Y_{100} to TAG
Forward: 5' – GACAAGGATGGTAATGGTTAGATTAGTGCTGCAGAACTTCG – 3'
Reverse: 5' – CGAAGTTCTGCAGCACTAATCTAACCATTACCATCCTTGTC – 3'

e. Mutation Y_{139} to F
Forward: 5' – AGACATTGATGGTGATGGTCAAGTAAACTTTGAAGAGTTTGTACA – 3'
Reverse: 5' – TGTACAAACTCTTCAAAGTTTACTTGACCATCACCATCAATGTCT – 3'

Figure S1. DNA oligomers for CaM Quikchange® mutagenesis.

Native PAGE Gel Analysis of CaM Mutants. CaM peptide binding can be detected by native (non-denaturing) PAGE gel analysis.[3] In order to determine whether mutant CaM was capable of binding peptide, 25 μL samples were prepared containing 10 μM of each CaM mutant, with or without a stoichiometric equivalent of pOCNC-F′$_1$. Prepared samples were then incubated for one hour at 4 °C and loaded into a non-denaturing gel with 2.5 μL of 60% glycerol and 2.5 μL of .01% bromophenol blue to assist loading. The gel was stained with Coomassie blue and scanned.

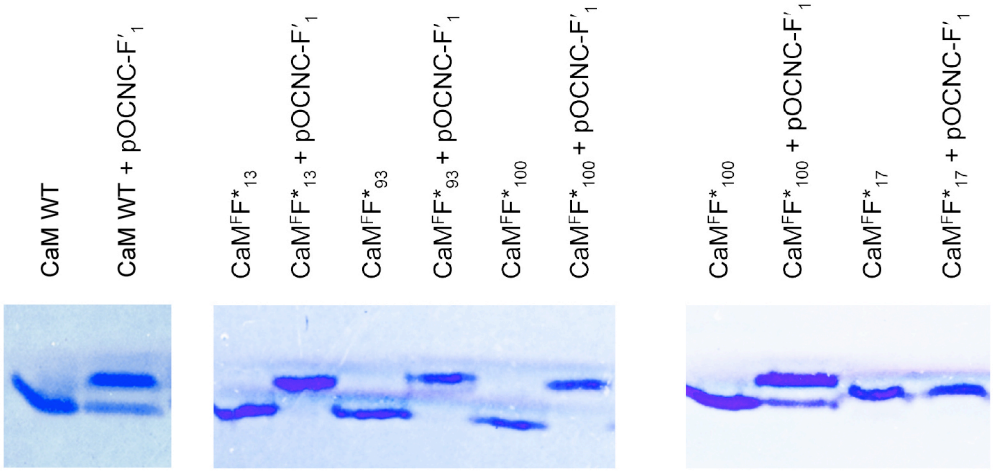

Figure S2. Native PAGE analysis of CaM WT and mutants. Left: PAGE analysis demonstrates upward shift of the CaM protein band upon addition of pOCNC-F′$_1$. No shift is observed upon addition of pOCNC-F′$_1$ to CaM^{F}F*$_{17}$, indicating this CaM mutant does not bind pOCNC-F′$_1$.

Calmodulin Circular Dichroism Measurements. Mutant stability was evaluated through both wavelength-dependent and temperature-dependent circular dichroism (CD) spectroscopy. The wavelength-dependent signature for both the calcium-containing CaM (holo CaM) and calcium-free CaM (apo CaM) was examined. Since holo CaM is thermostable, only the thermal unfolding of apo CaM was determined. The apo form of the protein was prepared by dialyzing the protein into 2 mM EDTA in 50 mM HEPES, pH 6.70. The holo form of the protein was prepared by dialyzing into 6 mM $CaCl_2$, 15 mM HEPES, 140 mM KCl, pH 6.70. Prepared samples containing 20 µM CaM were monitored at 222 nm between 5 and 95 °C using the variable temperature module for temperature-dependent scans and between 200 and 300 nm at room temperature for wavelength-dependent scans. Data were collected with a 1 °C/min slope, 30 s averaging time, 2 min temperature equilibration, 5 s response, and 1 nm band width. The data were processed as previously described.[4]

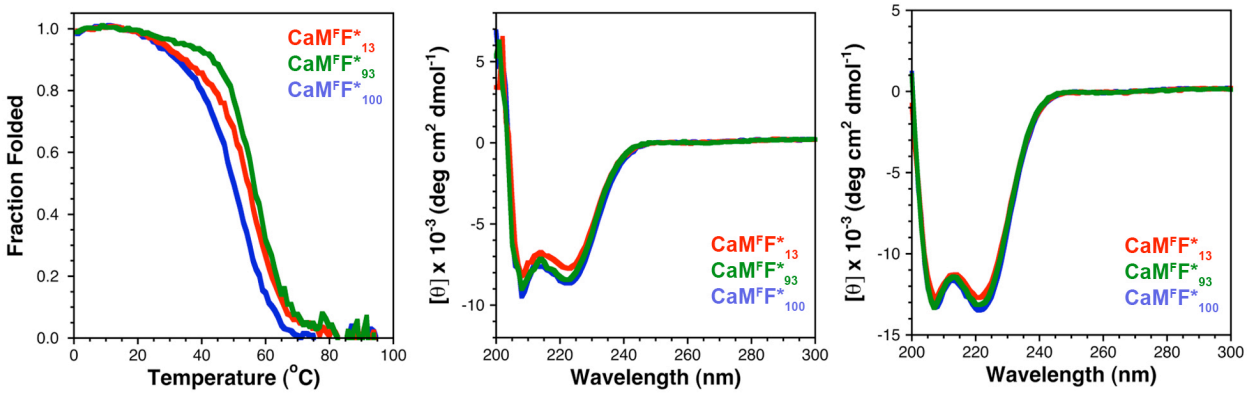

Figure S3. Temperature and wavelength-dependent circular dichroism measurements of CaM Mutants. Left: Temperature-dependent trace shown for apo CaM mutants. Middle: Wavelength-dependent trace (25 °C) shown for apo CaM mutants. Right: Wavelength-dependent trace (25 °C) shown for holo CaM mutants. Coloring scheme for all three plots $CaM^{F}F^{*}_{13}$ (red), $CaM^{F}F^{*}_{93}$ (green), $CaM^{F}F^{*}_{100}$ (blue).

Fluorescence Spectroscopy. Corrected fluorescence spectra were collected in triplicate using quartz fluorometer cells with path lengths of 1.00 cm. For all Cnf experiments, the excitation wavelength was 240 nm and emission data was collected from 275 - 400 nm as the average of three scans. The excitation and emission slit widths were 5 nm, the scan rate was 120 nm/min, the averaging time 0.5 s, and the data interval 1.0 nm.

CaM/pOCNC Binding Assays. Titration assays were performed by preparing individual samples containing increasing concentrations of each pOCNC peptide with each CaM mutant as described in the main text.

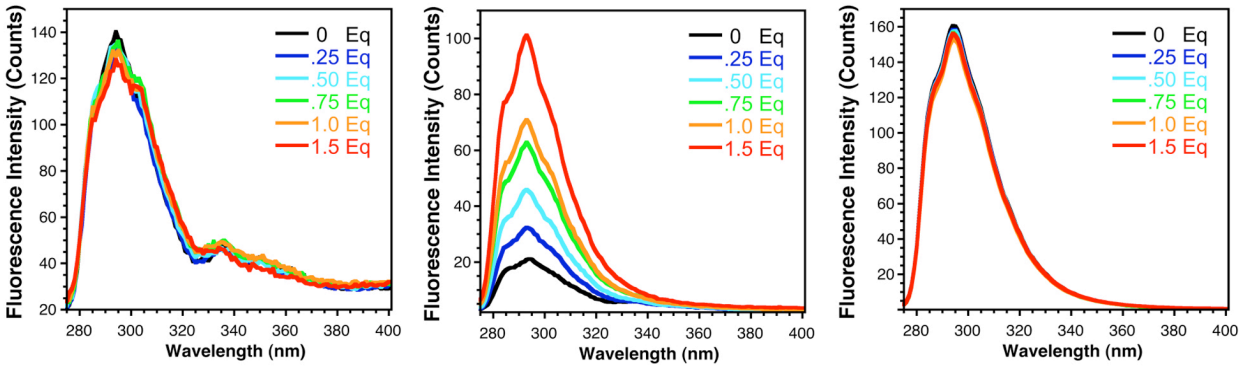

Figure S4. Fluorescence scans of pOCNC binding with CaM mutants. Left: $CaM^{F}F^{*}_{13}$, Middle: $CaM^{F}F^{*}_{93}$, Right: $CaM^{F}F^{*}_{100}$.

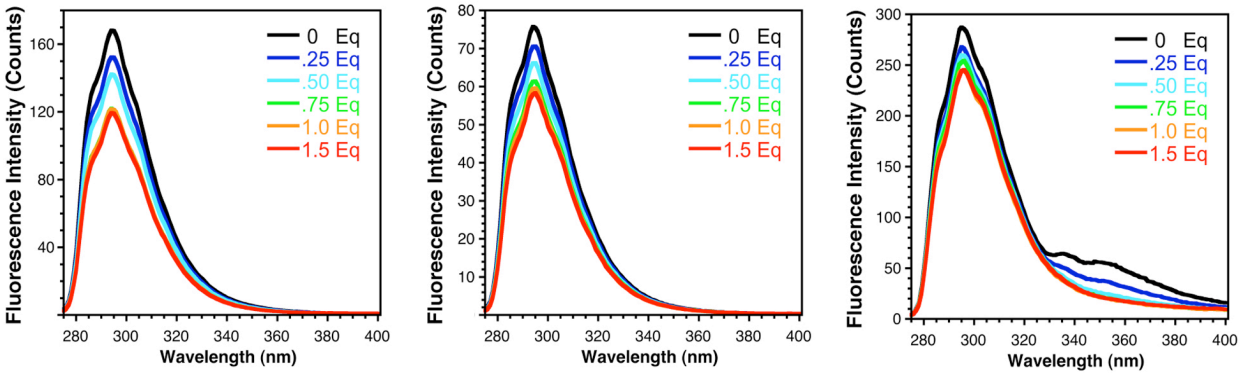

Figure S5. Fluorescence scans of thioamide pOCNC mutants binding with $CaM^{F}F^{*}_{100}$. Left: pOCNC-F'_{1}, Middle: pOCNC-L'_{11}, Right: pOCNC-F'_{16}.

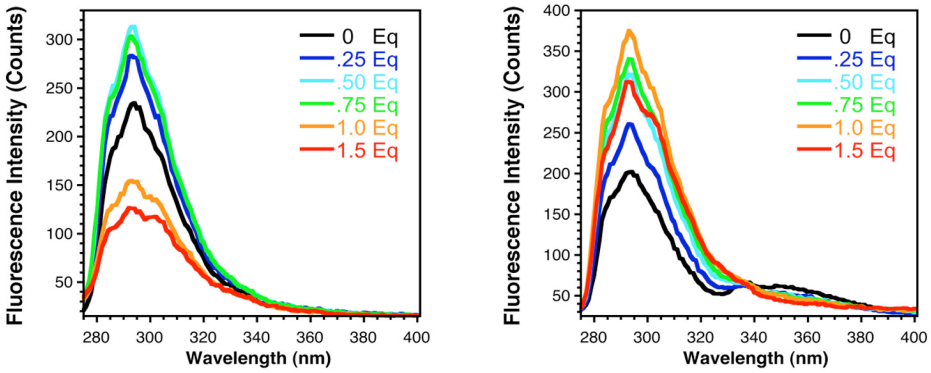

Figure S6. Fluorescence scans of pOCNC mutants binding with $CaM^{F}F^{*}_{93}$. Left: pOCNC-F'_{1}, Right: pOCNC-L'_{11}.

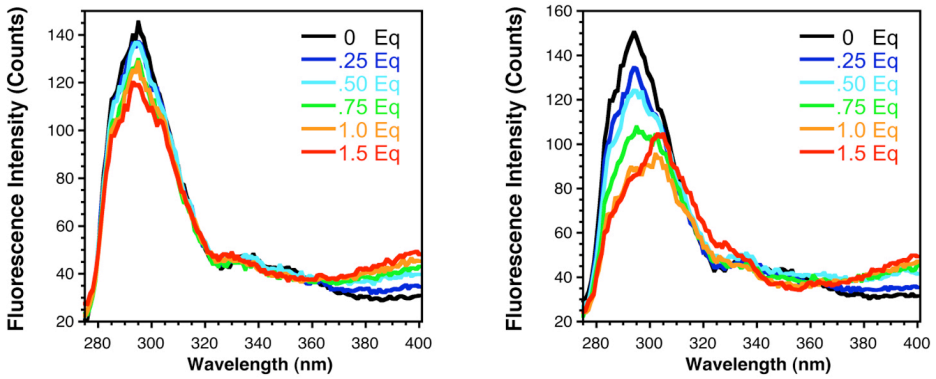

Figure S7. Fluorescence scans of pOCNC thioamide mutants Binding with $CaM^{F}F^{*}_{13}$. Left: pOCNC-F'_{1}, Right: pOCNC-L'_{11}.

Titration Analysis of Binding Studies with CaM Mutants. Normalized titration curves were obtained by plotting the ratio of the fluorescence of thioamide pOCNC complexes to the corresponding oxoamide pOCNC complexes (both measured at 295 nm) as a function of CaM/pOCNC ratio.

19 Å

24 Å

31 Å

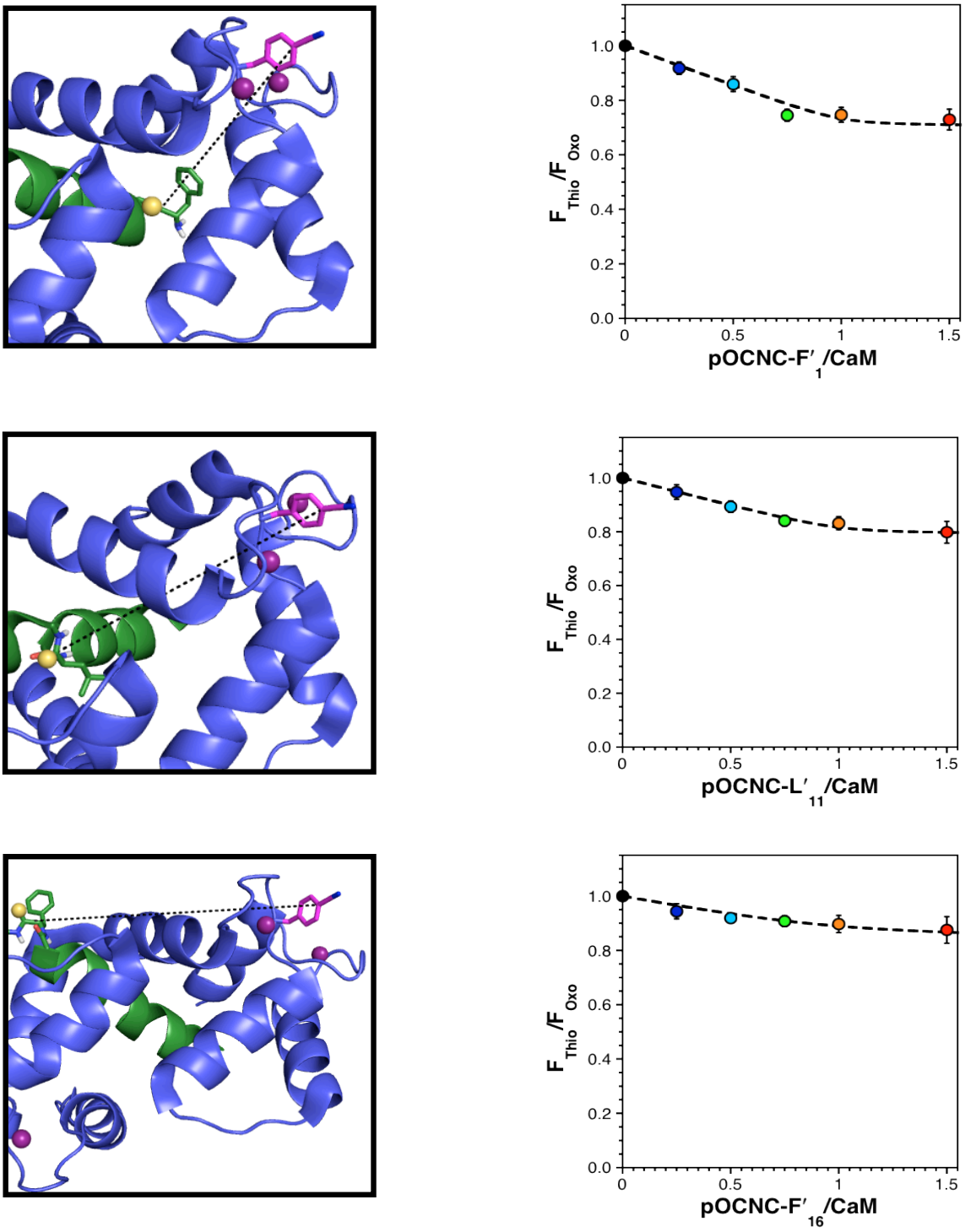

Figure S8. Binding of thioamide-containing-pOCNC with CaM^{F}F*$_{100}$. In each set, Left: Pymol figure illustrating the distance between the chromophores. Right: titration data for the binding experiment. Top: pOCNC-F′$_1$, Middle: pOCNC-L′$_{11}$, Bottom: pOCNC-F′$_{16}$.

12 Å 9 Å

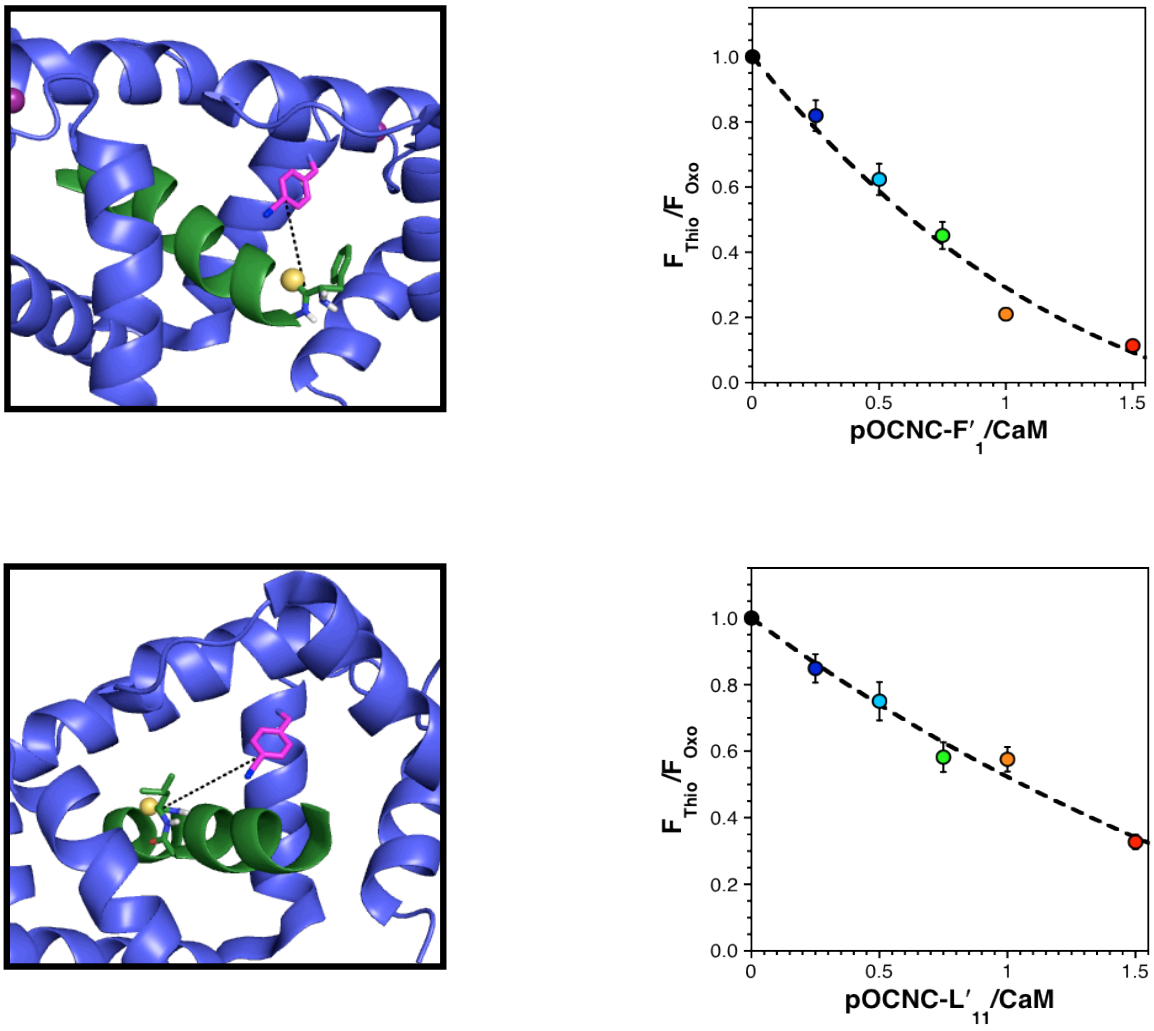

Figure S9. Binding of thioamide-containing-pOCNC with $CaM^{F}F^{*}_{93}$. In each set, Left: Pymol figure illustrating the distance between the chromophores. Right: titration data for the binding experiment. Top: pOCNC-F′$_1$, Bottom: pOCNC-L′$_{11}$.

14 Å

14 Å

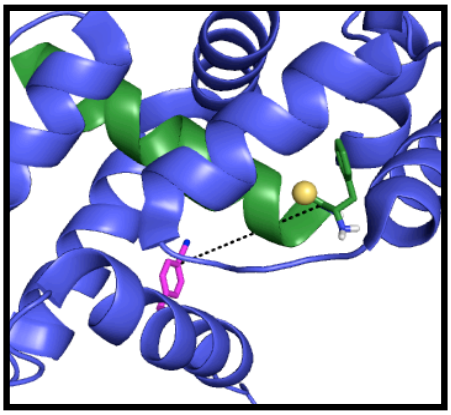

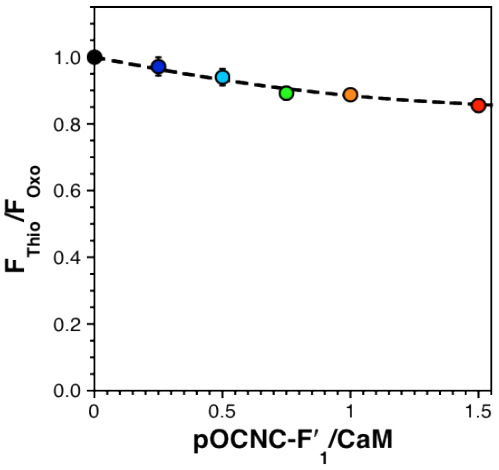

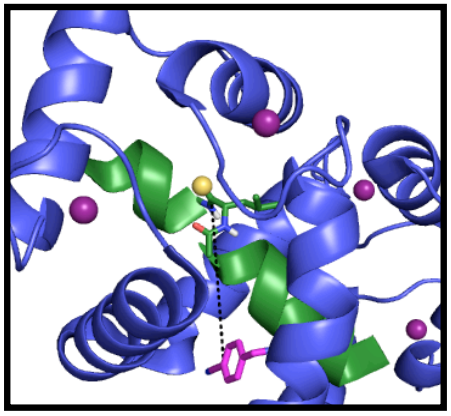

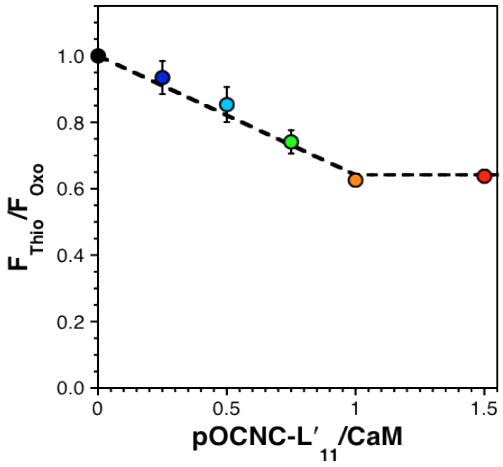

Figure S10. Binding of thioamide-containing-pOCNC with $CaM^{F}F^{*}_{13}$. In each set, Left: Pymol figure illustrating the distance between the chromophores. Right: titration data for the binding experiment. Top: pOCNC-F′$_1$, Bottom: pOCNC-L′$_{11}$.

Experimental Förster Distance Calculations (CaM). The Förster distance, R_0, is given in Å by equation (S1)

$$R_0^6 = \frac{9000(\ln 10)\kappa^2 Q_D J}{128\pi^5 n^4 N_A} \quad \text{(S1)}$$

where κ^2 is a geometrical factor that relates the orientation of the donor and acceptor transition moments, Q_D is the quantum yield of the donor, n is the index of refraction of the solvent, N_A is Avogadro's number, and J is the spectral overlap integral defined in units of $M^{-1}\bullet cm^{-1}\bullet nm^4$.[5,6] Combining constants and rearranging gives R_0 as

$$R_0 = 0.211\{Q_D\kappa^2 n^{-4} J\}^{1/6} \quad \text{(S2)}$$

J is formally defined as

$$J = \int_0^\infty f_D(\lambda)\varepsilon_A(\lambda)\lambda^4 d\lambda \quad \text{(S3)}$$

where $\varepsilon_A(\lambda)$ is the molar extinction coefficient of the acceptor at each wavelength λ and $f_D(\lambda)$ is the normalized donor emission spectrum given by

$$f_D(\lambda) = \frac{F_{D\lambda}(\lambda)}{\int_0^\infty F_{D\lambda}(\lambda) d\lambda} \quad \text{(S4)}$$

where $F_{D\lambda}(\lambda)$ is the fluorescence of the donor at each wavelength λ. J was calculated to be $7.0\times10^{12} \pm 2\times10^{11}$ $M^{-1}\bullet cm^{-1}\bullet nm^4$ as previously described.[7] Substituting this result into equation (S1), as well as 0.11 for the quantum yield of Cnf, 1.33 for the index of refraction of water, and 2/3 for κ^2 gives R_0 = 15.6 Å for Cnf/thioamide FRET pairs with Cnf at position 100 in CaM.[8] For Cnf/thioamide FRET pairs with Cnf at position 13 in CaM, we use 0.003 as a quantum yield for Cnf, and calculate R_0 = 8.6 Å. For Cnf/thioamide FRET pairs with Cnf at position 93 in

CaM, we use 0.014 as a quantum yield for Cnf, and calculate R_0 = 11.1 Å. Quantum yields for each mutant were determined by comparing the fluorescence output of the mutant relative to the fluorescence of $CaM^{F}F^{*}_{100}$ under oxopeptide (pOCNC) bound conditions using identical concentrations and fluorometer settings. Comparison of $CaM^{F}F^{*}_{100}$ fluorescence to free Cnf showed that no substantial quenching occurred in this mutant in the absence of thiopeptide (data not shown).

These values of R_0 were then used in determining experimental chromophore separations (R_{FRET}) for each set of Cnf/thioamide probe locations according to equation (S5)

$$R_{FRET} = R_0\left(\frac{1}{E_Q} - 1\right)^{1/6} \quad \text{(S5)}$$

where E_Q is defined by equation (S6) as described in the main text.

$$E_Q = 1 - (F_{Thio}/F_{Oxo}) \quad \text{(S6)}$$

The resulting R_{FRET} values are shown in Table 1 in the main text.

Chromophore Geometries from CaM/pOCNC NMR Structure. For each pair of Cnf donor and thioamide acceptor locations, the corresponding residues were identified in the 1SYD PDB file, and a Tcl script was run in VMD (http://www.ks.uiuc.edu/) to cull distance and orientation information for the Cnf ring (using the corresponding positions in the natural Phe or Tyr in 1SYD) and the thioamide Xxx′ carbonyl (using the corresponding positions in the given amide backbone unit in 1SYD).[9] The following positions were determined in accordance with the vectors identified in previous quantum mechanical calculations: the midpoint between CE1 and CE2 (CEmp) of Cnf as a proxy for the center of the Cnf transition dipole; the midpoint between Xxx′ C and N of the next amino acid (CNmp) as a proxy for the midpoint of the thioamide dipole.[7] The interchromophore distance (R_{NMR}) was determined as the distance between these two midpoints. The culled data were also used to calculate theoretical FRET efficiencies for each set of probe locations. The donor-acceptor dihedral angle (ϕ_{DA}) was determined as the Xxx′ O, CNmp, CEmp, Phe CE2 dihedral angle. The donor angle (θ_D) was determined as the Xxx′ O, CNmp, CEmp angle; and acceptor angle (θ_A) was determined as the CNmp, CEmp, CE2 angle. These parameters are illustrated in Figure S11.

$R_{CNmp/CEmp}$ = 19.3 Å
θ_D = 114.7°
θ_A = 67.5°
ϕ_{DA} = 91.4°

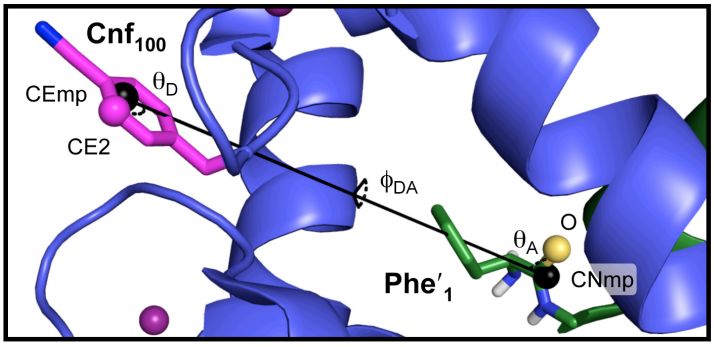

Figure S11. FRET Orientational Parameters. Structure 1 from PDB 1SYD shown with atoms used in determining κ^2 and relevant distances and angles illustrated. CNmp and CEmp indicated by black spheres. Shown with nitrile and thioamide modifications for clarity, although geometry calculations are identical for unmodified 1SYD file.

The orientational parameter from Förster theory, κ^2, was calculated as:

$$\kappa^2 = (\sin\theta_D \sin\theta_A \cos\phi_{DA} - 2\cos\theta_D \cos\theta_A)^2 \quad \text{(S7)}$$

where ϕ_{DA}, θ_D, and θ_A are defined as above.[6] Geometry-specific R_0 values were calculated for each of the twenty structures in PDB 1SYD using equations (S2) and (S3) where the donor quantum yield (Q_D) is taken as 0.11, the spectral overlap integral (J) is calculated as above, and the index of refraction (n) is taken as 1.33.[8] For each timestep, this value of R_0 was used to calculate a geometry-specific FRET quenching efficiency (E_Q) using the corresponding donor-acceptor separation, R_{NMR} (the CNmp/CEmp distance). E_Q was calculated using equation (S6). Values averaged over all 20 structures in PDB 1SYD for R_{NMR}, κ^2, R_0, and E_Q are collected in Table S4. These R_{NMR} values are listed in Table 1 in the main text.

Table S4. Orientation Parameters and Theoretical E_{FRET} from CaM/pOCNC NMR Structures[a]

CaM_F_{13}/pOCNC_F_1 (Φ = 0.003)	R_{NMR}	κ^2	R_0	E_Q
Average	14.1	1.01	8.0	0.07
RMSD	0.3	0.63	1.5	0.04
CaM_F_{13}/pOCNC_L_{11} (Φ = 0.003)	R_{NMR}	κ^2	R_0	E_Q
Average	14.1	0.92	8.1	0.07
RMSD	0.4	0.47	1.3	0.03
CaM_F_{93}/pOCNC_F_1 (0.014)	R_{NMR}	κ^2	R_0	E_Q
Average	8.9	1.12	11.1	0.73
RMSD	0.3	0.58	1.4	0.14
CaM_F_{93}/pOCNC_L_{11} (0.014)	R_{NMR}	κ^2	R_0	E_Q
Average	12.2	1.19	10.8	0.39
RMSD	0.5	0.68	1.8	0.15
CaM_F_{100}/pOCNC_F_1 (0.110)	R_{NMR}	κ^2	R_0	E_Q
Average	18.9	1.30	16.2	0.32
RMSD	0.3	0.57	2.1	0.11
CaM_F_{100}/pOCNC_L_{11} (0.110)	R_{NMR}	κ^2	R_0	E_Q
Average	24.4	1.02	15.2	0.09
RMSD	0.4	0.58	2.2	0.04
CaM_F_{100}/pOCNC_F_{16} (0.110)	R_{NMR}	κ^2	R_0	E_Q
Average	31.3	1.05	14.6	0.02
RMSD	0.7	0.68	2.8	0.01

[a] Parameters calculated as described in Supporting Information text. All distances in Å.

Epimer Analysis of pOCNC-F′$_{16}$. Upon purification of pOCNC-F′$_{16}$, two distinct peaks were observed with different retention times. We attribute this to epimerization resulting from a reversible cyclization reaction similar to the Edman degradation reaction. Both peaks contained the correct mass of pOCNC-F′$_{16}$ by MALDI MS. The fluorescence titration assay was performed with a combination of both epimers of the peptide. To confirm that both epimers bound CaM^{F}F*$_{100}$, a native PAGE gel was run with and without each epimer of pOCNC-F′$_{16}$ as described previously.

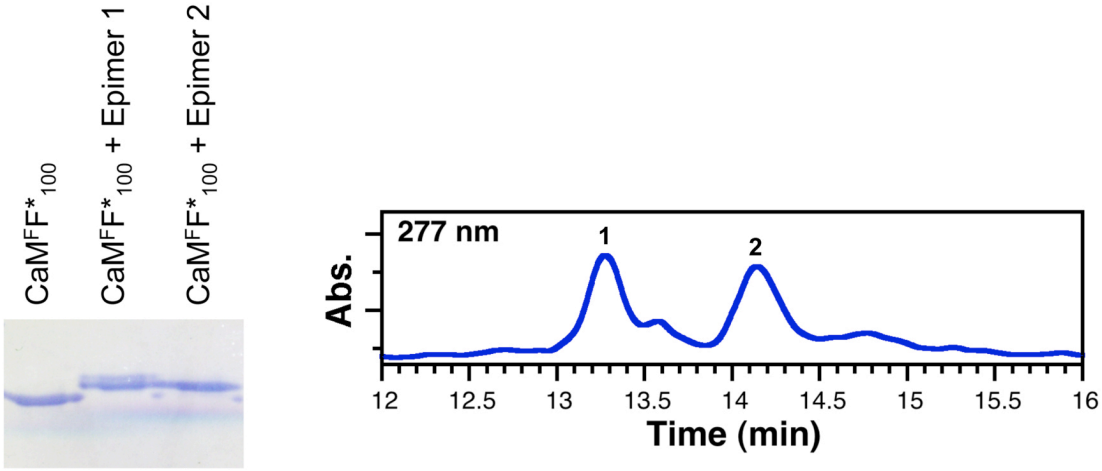

Figure S12. Native PAGE and HPLC analysis of pOCNC-F′$_{16}$. Left: Gel analysis shows shift upon addition of each epimer of pOCNC-F′$_{16}$ to CaM^{F}F*$_{100}$, indicating binding. Right: HPLC purification trace at 277 nm. Peaks **1** and **2** correspond to the peptide epimers.

αS Peptide Synthesis and Purification. Peptide synthesis was performed as described in the main text. αS peptide fragments were synthesized on chlorotrityl resin. Peptides were purified by HPLC using a binary system of Buffer A and Buffer B. Thioesterification was performed as described in the main text. Solvent gradients, column descriptions, and retention times are listed in Tables **S5** and **S7**. Purified peptides were lyophilized or dried in a vacuum centrifuge. Purified proteins were exchanged into Tris buffer (20 mM Tris, 100 mM NaCl, pH 7.4).

Table S5. Summary of HPLC Purified Peptides and Proteins.

Peptide	Gradient Description†	Retention Time (min)	Column (Size: Brand)
Ac-MDVF'MKGL-S$(CH_2)_2CO_2$Me	S3	24.1	Semi-prep: YMCBasic C8
Ac-MDV'FMKGL-C^bPG_o	S4	31.9	Semi-prep: Vydac 218 TP C18
$\alpha S_{123\text{-}140}C_{123}A'_{124}$	S5	20.5	Prep: Waters C18
Ac-$\alpha S^F F'_4 C_9 F^*_{39}$	S6	31.5	Semi-prep: Vydac 218 TP C4
Ac-$\alpha S^F F'_4 C_9 F^*_{94}$	S6	28.9	Semi-prep: Vydac 218 TP C4
$\alpha S^F F^*_{39} C_{123} A'_{124}$	S7	28.9	Semi-prep: Vydac 218 TP C4
Ac-$\alpha S^F V'_3 C_9 F^*_{39}$	S6	29.5	Semi-prep: Vydac 218 TP C4

Table S6. Calculated and Observed Peptide and Protein Masses.

Peptide	Calculated m/z $[M+H]^+$	Observed m/z $[M+H]^+$	Calculated m/z $[M+Na]^+$	Observed m/z $[M+Na]^+$
Ac-MDVF'MKGL-S$(CH_2)_2CO_2$Me	1101.38	1101.43	1123.36	---
Ac-MDV'FMKGL-C^bPG_o	1343.56	1343.91	1366.54	1365.89
$\alpha S_{123\text{-}140}C_{123}A'_{124}$	2078.86	2078.73	2100.66	2100.69
$\alpha S^F C^9 F^*_{39}$	14438.1	14437.6	14461.1	---
$\alpha S^F C^9 F^*_{94}$	14438.1	14439.6	14461.1	---
$\alpha S^F F^*_{39} C_{123}$	14386.1	---	14409.1	14411.3
$\alpha S^F_{\Delta 1\text{-}8} C_9 F^*_{39}$	13516.0	13517.2	13534.0	---
Ac-$\alpha S^F F'_4 C_9 F^*_{39}$	14494.7	14495.7	14517.7	---
Ac-$\alpha S^F F'_4 C_9 F^*_{94}$	14494.7	14495.9	14517.7	---
Ac-$\alpha S^F V'_3 C_9 F^*_{39}$	14494.7	14495.4	14517.7	---
$\alpha S_{1\text{-}122} F^*_{39} SR$	12475.2	12475.5	12497.2	---
$\alpha S^F F^*_{39} C_{123} A'_{124}$	14412.2	14412.5	14434.2	---

Table S7. Solvent Gradients Used for Peptide Purification and Analysis.

Gradient	Time (min)	Buffer A (%)	Gradient	Time (min)	Buffer A (%)
S3	0:00	98	S4	0:00	98
	5:00	98		5:00	98
	10:00	85		10:00	75
	30:00	65		25:00	40
	35:00	0		30:00	0
	40:00	0		35:00	0
	45:00	98		40:00	98
S5	0:00	95	S6	0:00	95
	5:00	95		5:00	95
	10:00	77		10:00	70
	27:00	60		30:00	40
	30:00	0		34:00	0
	35:00	0		38:00	0
	40:00	98		43:00	95
S7	0:00	95			
	5:00	95			
	10:00	70			
	30:00	50			
	34:00	0			
	38:00	0			
	43:00	95			

Construction of Recombinant pET16b αS Expression Plasmids. The generation of pET16b-His_{11}IEGR-$\alpha S_{\Delta 1\text{-}8}C_9$ has been described previously.[10] All tyrosine residues (Y_{39}, Y_{125}, Y_{133}, and Y_{136}) were mutated to phenylalanine by multiple rounds of QuikChange® mutagenesis to generate pET16b-His_{11}IEGR-$\alpha S^{F}_{\Delta 1\text{-}8}C_9$. The amber stop codon (TAG) was subsequently mutated into the pET16b-His_{11}IEGR-$\alpha S^{F}_{\Delta 1\text{-}8}C_9$ construct at nucleotides corresponding to position 39 or 94 to generate pET16b-His_{11}IEGR-$\alpha S^{F}_{\Delta 1\text{-}8}C_9TAG_{39}$ and pET16b-His_{11}IEGR-$\alpha S^{F}_{\Delta 1\text{-}8}C_9TAG_{94}$.

Construction of Recombinant pRK127 αS Expression Plasmids. A plasmid containing the human wild-type αS gene cloned between NdeI and HindIII in the expression vector pRK172 was provided by Dr. Virginia Lee (Perelman School of Medicine, University of Pennsylvania). All tyrosine residues were mutated to phenylalanine by multiple rounds of Quikchange® mutagenesis to generate pRK172-αS^{F}. The amber stop codon (TAG) was subsequently mutated into the pRK172-αS^{F} construct at nucleotides corresponding to amino acid position 39 or 94 to generate pRK172-$\alpha S^{F}TAG_{39}$ and pRK172-$\alpha S^{F}TAG_{94}$. In order to create N-terminal cysteine constructs for native chemical ligation, a primer was designed to delete nucleotides corresponding to amino acids 2-8 while simultaneously mutating Ser_9 to Cys. This primer was applied to pRK172-$\alpha S^{F}TAG_{39}$ and pRK172-$\alpha S^{F}TAG_{94}$ to generate pRK172-$\alpha S^{F}_{\Delta 2\text{-}8}C_9TAG_{39}$ and pRK172-$\alpha S^{F}_{\Delta 2\text{-}8}C_9TAG_{94}$ (Figure S13). Ser_9 was mutated to Cys in all full-length oxoamide control constructs to yield pRK172-$\alpha S^{F}C_9TAG_{39}$ and pRK172-$\alpha S^{F}C_9TAG_{94}$.

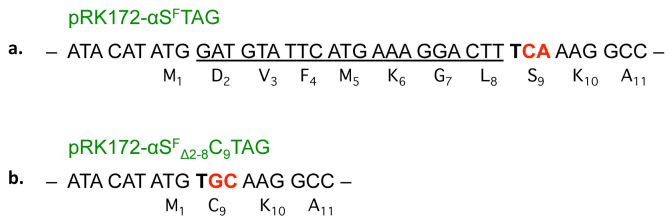

Figure S13. Construction of pRK172-$aS^{F}_{\Delta 2\text{-}8}C_9TAG$ mutants. A primer was designed to delete nucleotides corresponding to amino acid residues 2-8 (underlined) and mutate S9 to C (bolded) with a single round of Quikchange$^{\Delta}$ mutagenesis.

Construction of Recombinant pTXB1-$\alpha S_{1\text{-}122}F^{*}_{39}$-$H_{Tag}$ Expression Plasmid. A plasmid containing a wild type αS gene was digested by NdeI and XhoI, gel-purified, and ligated into NdeI/XhoI site of the pTXB1 vector which contained mini-intein GyrA from the *Mycobacterium*

xenopi followed by a chitin binding domain (CBD). An XhoI site (CTCGAG) was introduced at D_{121}/N_{122} of αS using QuikChange® mutagenesis . Digestion with XhoI and ligation of the two sticky ends yielded a pTXB1-$\alpha S_{1\text{-}122}D_{121}L\text{-}N_{122}E$-SapI site plasmid. Finally, QuikChange® mutagenesis was used to mutate $L_{121}D$ and $N_{122}E$ while simultaneously deleting the SapI site for generating pTXB1-$\alpha S_{1\text{-}122}$ plasmid.

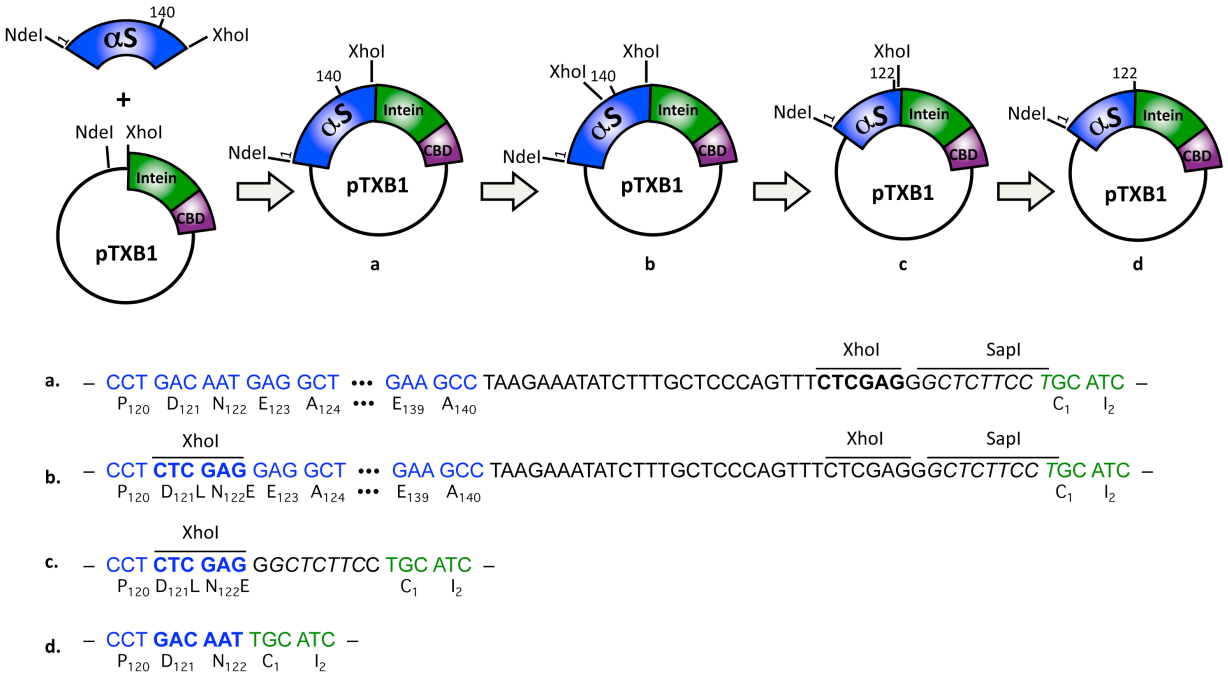

Figure S14. Construction of $\alpha S_{1\text{-}122}$ intein expression plasmid with C-terminal chitin binding domain.

To replace CBD with a polyhistidine tag at the C-terminus of the intein, two HindIII sites were introduced at the N- and C- termini of CBD using QuikChange® mutagenesis. The main portion of the CBD was removed by digestion with HindIII and ligation of the two sticky ends. Then, six His were inserted between the HindIII and stop codon. The plasmid sequence was confirmed by sequencing using T7-promotor as well as T7-terminator primers. Lastly, the amber stop codon (TAG) was introduced at position 39 using QuikChange® mutagenesis to generate $\alpha S^{F}_{1\text{-}122}TAG_{39}$-Int construct.

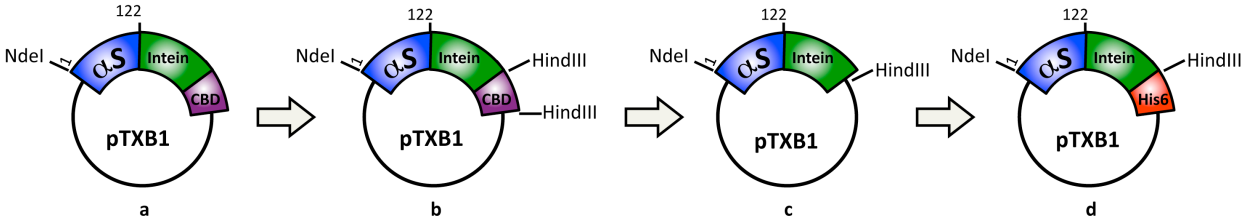

a. – CCT GAC AAT TGC ATC ••• GCT ACT GGC CTC ACC GGT CTG AAC TCA GGC ••• CTT CAA TGA
P_{120} D_{121} N_{122} C_1 I_2 ••• A_{197} T_{198} G_1 L_2 T_3 G_4 L_5 N_6 S_7 G_8 ••• L_{49} Q_{50} STOP

b. – CCT GAC AAT TGC ATC ••• GCT ACT GGC CTC ACC GGT CTG **AAG CTT** GGC ••• **AAG CTT** TGA (HindIII, HindIII)
P_{120} D_{121} N_{122} C_1 I_2 ••• A_{197} T_{198} G_1 L_2 T_3 G_4 L_5 N6K S7L G_8 ••• L49K Q50L STOP

c. – CCT GAC AAT TGC ATC ••• GCT ACT GGC CTC ACC GGT CTG **AAG CTT** TGA (HindIII)
P_{120} D_{121} N_{122} C_1 I_2 ••• A_{197} T_{198} G_1 L_2 T_3 G_4 L_5 N6K S7L STOP

d. – CCT GAC AAT TGC ATC ••• GCT ACT GGC CTC ACC GGT CTG AAG CTT **CAT CAT CAT CAT CAT CAT** TAA TGA
P_{120} D_{121} N_{122} C_1 I_2 ••• A_{197} T_{198} G_1 L_2 T_3 G_4 L_5 N6K S7L H H H H H H STOP STOP

Figure S15. Construction of $\alpha S_{1\text{-}122}$ intein expression plasmid with C-terminal His_6 tag.

DNA Oligomers Used for αS QuikChange ® Mutagenesis

a. Mutation $Y_{39}F$
Forward: 5' – GGAAAGACAAAAGAGGGTGTTCTCTTTGTAGGCTCCAAA – 3'
Reverse: 5' – TTTGGAGCCTACAAAGAGAACACCCTCTTTTGTCTTTCC – 3'

b. Mutation $Y_{125}F$
Forward: 5' – GGATCCTGACAATGAGGCTTTTGAAATGCCTTCTGA – 3'
Reverse: 5' – TCAGAAGGCATTTCAAAAGCCTCATTGTCAGGATCC – 3'

c. Double Mutation $Y_{133}F\_Y_{136}F$
Forward: 5' – CCTTCTGAGGAAGGGTTTCAAGACTTCGAACCTGAAGCC – 3'
Reverse: 5' – GGCTTCAGGTTCGAAGTCTTGAAACCCTTCCTCAGAAGG – 3'

d. Mutation $Y_{39}TAG$
Forward: 5' – AAAAGAGGGTGTTCTCTAGGTAGGCTCCAAAACCAA – 3'
Reverse: 5' – CTTGGTTTTGGAGCCTACCTAGAGAACACCCTCTTTT – 3'

e. Mutation $F_{94}TAG$
Forward: 5' – GCATTGCAGCAGCCACTGGCTAGGTCAAAAAGGACCAGTTGGG – 3'
Reverse: 5' – CCCAACTGGTCCTTTTTGACCTAGCCAGTGGCTGCTGCAATGC – 3'

e. Deletion 2-8 and Mutation S_9C
Forward: 5' – AGAAGGAGATATACATATGTGCAAGGCCAAGGAGGG – 3'
Reverse: 5' – CTCCCTCCTTGGCCTTGCACATATGTATATCTCCTTCT – 3'

f. XhoI site introduction at D_{121}/N_{122}
Forward: 5' – GGAAGATATGCCTGTGGATCCTCTCGAGGAGGCTTATGAAATGCCTTCTG – 3'
Reverse: 5' – CAGAAGGCATTTCATAAGCCTCCTCGAGAGGATCCACAGGCATATCTTCC – 3'

g. Mutation $L_{121}D/E_{122}N$ and deletion of SapI site
Forward: 5' – GGAAGATATGCCTGTGGATCCTGACAATTGCATCACGGGAGATGCA– 3'
Reverse: 5' – TGCATCTCCCGTGATGCAATTGTCAGGATCCACAGGCATATCTTCC – 3'

h. Insertion of HindIII – 1^{st} site
Forward: 5' – TACTGGCCTCACCGGTCTGAAGCTTGGCCTCACGACAAATCC – 3'
Reverse: 5' – GGATTTGTCGTGAGGCCAAGCTTCAGACCGGTGAGGCCAGTA – 3'

i. Insertion of HindIII – 2^{nd} site
Forward: 5' – CGTTCCTGCCTTGTGGCAGAAGCTTTGACTGCAGGAAGGGGATCC – 3'
Reverse: 5' –GGATCCCCTTCCTGCAGTCAAAGCTTCTGCCACAAGGCAGGAACGT – 3'

j. Introduction of His Tag
Forward: 5' – CTCACCGGTCTGAAGCTTCATCATCATCATCATCATTAATGACTGCAGGAAGGG – 3'
Reverse: 5' –CCCTTCCTGCAGTCATTAATGATGATGATGATGATGAAGCTTCAGACCGGTGAG – 3'

Figure S16. DNA oligomers used for αS mutagenesis.

Generation of pDule2-Cnf-BL21(DE3) *E. Coli* Cells for Unnatural Amino Acid Mutagenesis. A plasmid encoding for an orthogonal $tRNA_{CUA}$ and pCnf-tRNA synthetase for the incorporation of pCnf through amber stop codon suppression (pDULE2-Cnf) was provided by Dr. Ryan Mehl (University of Oregon).[11] *E. coli* BL21(DE3) cells were transformed with this plasmid and plated onto LB agar plates containing streptomycin. Following transformation, competent cells for protein expression were brewed in accordance with the Hanahan method.[11] Cells stocks were stored at - 80 °C in single-use aliquots.

Overexpression and Purification of Full-length αS Cnf Mutants. $\alpha S^{F}C_{9}F^{*}_{39}$, $\alpha S^{F}C_{9}F^{*}_{94,}$ and $\alpha S^{F}F^{*}_{39}C_{123}$ were transformed into competent *E. coli* BL21(DE3) cells harboring the orthogonal $tRNA_{CUA}$ and pCnf-tRNA synthetase pair. Transformed cells were selected on the basis of ampicillin (Amp) and streptomycin (Strep) resistance. Single colonies were used to inoculate 5 mL of LB media supplemented with Amp (100 ug/mL) and Strep (100 ug/mL). The primary 5 mL culture was incubated at 37 °C with shaking at 250 rpm for 5 hours. The primary culture was used to inoculate 1 L of a variant of M9 minimal media. To an autoclaved 1L solution containing 6 g Na_2HPO_4, 3 g KH_2PO_4, .5 g NaCl and 1 g NH_4Cl, the following autoclaved solutions were added: 1 mL of 2 M $MgSO_4$, 1 mL of 15 mg/mL $FeCl_2$ (in 1.0 M HCl), 1 mL of 15 mg/mL $ZnCl_2$ (in acidified H_2O), 2 mL of 10% Bacto™ Yeast Extract 6.5 mL 40% glucose (w/v), and 1 μL of 1 M $CaCl_2$. When the OD_{600} of the secondary culture reached 0.8, Cnf was added (100 mg, 0.5 mM final concentration), and the culture was incubated overnight at 37 °C with shaking at 250 rpm. The cells were harvested at 5000 x g for 15 min and the resulting pellet was resuspended in 20 mM Tris, pH 8. Following sonication, the cell lysate was boiled for 20 minutes prior to centrifugation for 20 minutes at 30,000 x g, 4 °C. The cleared lysate was dialyzed against 20 mM Tris pH 8.0, loaded onto a Superdex 200 column (25 cm)

connected to a BioCad Sprint (FPLC) system and eluted with 20 mM Tris, pH 8. FPLC fractions post size-exclusion chromatography were analyzed by SDS PAGE. The fractions containing αS were then loaded onto a HighTrap Q HP column and eluted over a 100 minute sodium chloride gradient (0 to 0.5M NaCl in 20 mM Tris, pH 8). FPLC fractions post ion-exchange chromatography were dialyzed against 20 mM Tris, 100 mM NaCl, pH 7.4 and analyzed by SDS PAGE, MALDI, and fluorescence spectroscopy.

Mass Spectrometry and Fluorescence Spectrum of $\alpha S^{F}C_9F^{*}_{39}$

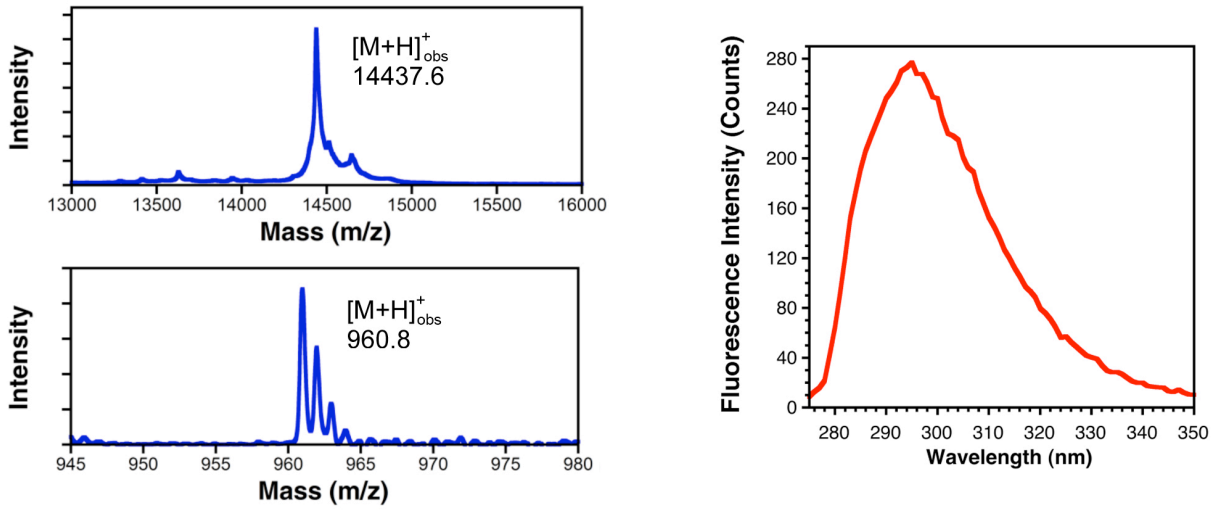

Figure S17. MALDI MS (top left), trypsin digestion (top right), and primary fluorescence (bottom) of full-length $\alpha S^{F}C_9F^{*}_{39}$ .Calcd m/z of $\alpha S^{F}C_9F^{*}_{39}$:14438.1 Calcd m/z of trypsin fragment 35-43: 961.1

Mass Spectrometry and Fluorescence Spectrum of $\alpha S^{F}C_9F^{*}_{94}$

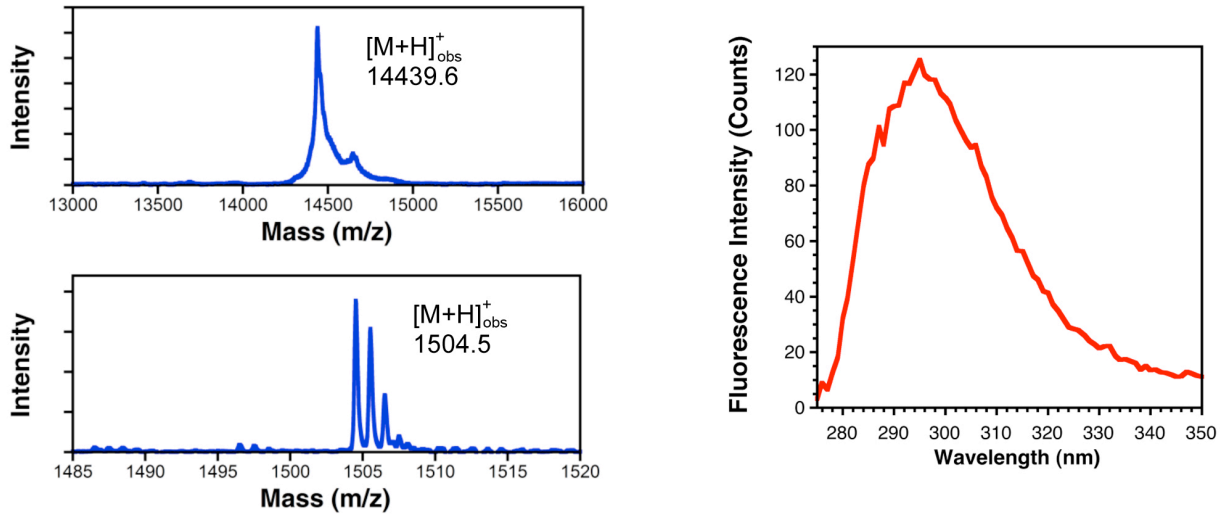

Figure S18. MALDI MS (top left), trypsin digestion (top right), and primary fluorescence (bottom) of full-length $\alpha S^{F}C_9F^{*}_{94.}$ Calcd m/z of $\alpha S^{F}C_9F^{*}_{94:}$ 14438.1 Calcd m/z of trypsin fragment 81-96: 1503.8.

Mass Spectrometry and Fluorescence Spectrum of $\alpha S^{F}F^{*}_{39}C_{123}$

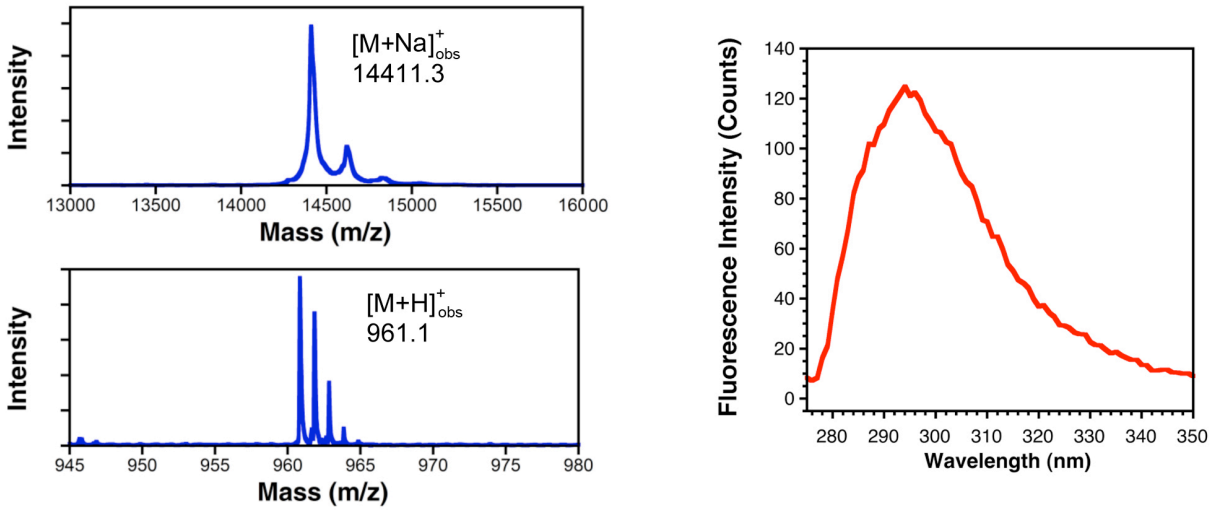

Figure S19. MALDI MS (top left), trypsin digestion (top right), and primary fluorescence (bottom) of full-length $\alpha S^{F}F^{*}_{39}C_{123}$. Calcd m/z of $\alpha S^{F}F^{*}_{39}C_{123}$: 14409.1 Calcd m/z of trypsin fragment 35-43: 961.1

Mass Spectrometry of $\alpha S^{F}_{\Delta 1\text{-}8}C_{9}F^{*}_{39}$ Generated by Met Aminopeptidase Cleavage. Deprotection of N-terminal cysteine adducts formed during protein expression was performed as described in the main text. Prior to deprotection, adducts corresponding to a mass increase of +26, +49, and +70 Da are observed. The reaction progress can be monitored by MALDI MS.

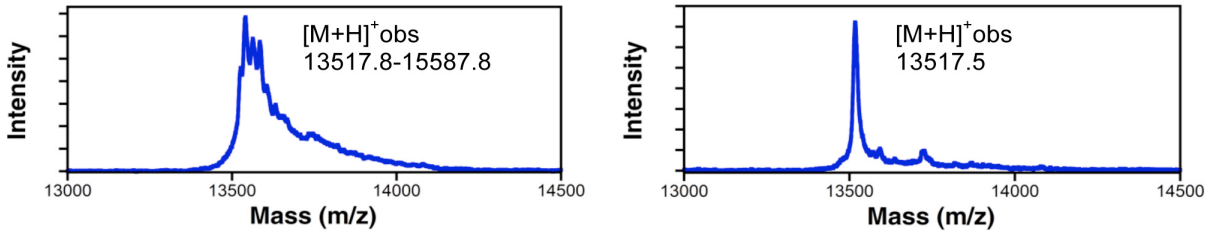

Figure S20. MALDI analysis pre (left) and post (right) overnight incubation with $MeONH_2$•HCl in 6M Gdn•HCl, pH 4.0, at 4 °C. Calcd m/z of $\alpha S^{F}_{\Delta 1\text{-}8}C_{9}F^{*}_{39}$: 13516.0

Mass Spectrometry of $\alpha S^{F}_{\Delta 1\text{-}8}C_9F^*_{39}$ Generated by Factor Xa Cleavage. Factor Xa-mediated cleavage of the N-terminal histidine tag followed by an IEGR recognition site was performed as described in the main text. Removal of the His tag was confirmed by MALDI MS.

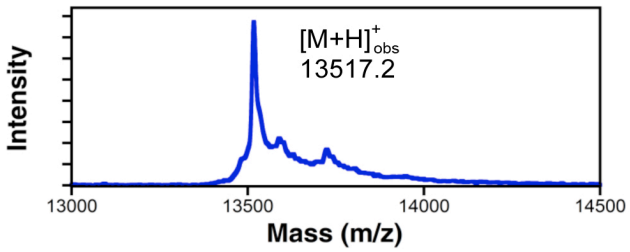

Figure S21. MALDI analysis of $\alpha S^{F}_{\Delta 1\text{-}8}C_9F^*_{39}$ post Factor Xa cleavage. Expected mass of $\alpha S^{F}_{\Delta 1\text{-}8}C_9F^*_{39}$ post cleavage: 13516.0

HPLC Analysis of Ac-$\alpha S^{F}F'_4C_9F^*_{39}$ and Ac-$\alpha S^{F}F'_4C_9F^*_{94}$ Ligations. Conditions for native chemical ligation reactions using mercaptopropionate thioester peptide formed by PyBOP activation were described in the main text. HPLC analyses of the ligation reactions were performed after 20 h.

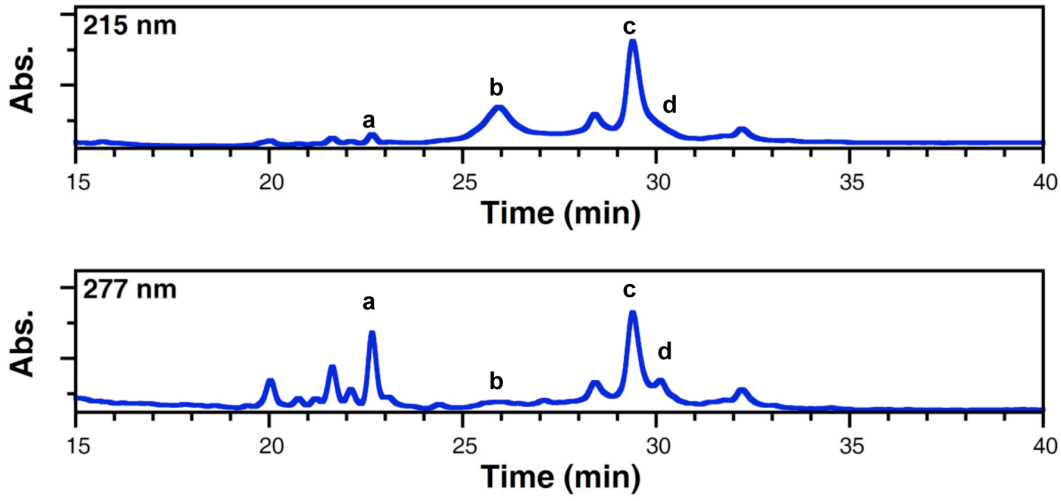

Figure S22. HPLC analysis of ligation of Ac-$\alpha S^{F}F'_4C_9F^*_{39}$. Peaks **a**, **b**, **c**, and **d** correspond to hydrolyzed Ac-$\alpha S_{1\text{-}8}F'_4$ thioester, $\alpha S^{F}_{\Delta 1\text{-}8}C_9F^*_{39}$, ligation product Ac-$\alpha S^{F}F'_4C_9F^*_{39}$, and intact Ac-$\alpha S_{1\text{-}8}F'_4$ thioester. Peaks earlier than **a** correspond to hydrolyzed peptide side products.

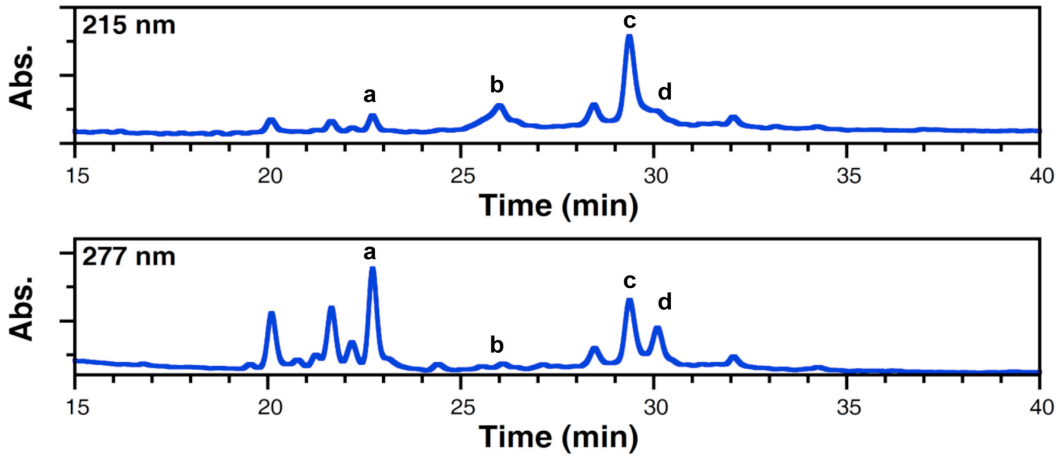

Figure S23. HPLC analysis of ligation of Ac-αS^{F}F′$_4$C$_9$F*$_{94}$. Peaks **a**, **b**, **c**, and **d** correspond to hydrolyzed Ac-αS$_{1\text{-}8}$F′4 thioester, αS$^{F}_{\Delta 1\text{-}8}$C$_9$F*$_{94}$, ligation product Ac-αS^{F}F′$_4$C$_9$F*$_{94}$, and intact Ac-αS$_{1\text{-}8}$F′4 thioester. Peaks earlier than **a** correspond to hydrolyzed peptide side products.

Conditions for native chemical ligation reactions using peptide thioester formed by *in situ* deprotection and rearrangement of the C^{b}PG$_o$ linker are described in the main text. HPLC analyses of the ligation reactions were performed after 20 h. Due to low yields of peptide synthesis, ligation reactions were not fully optimized.

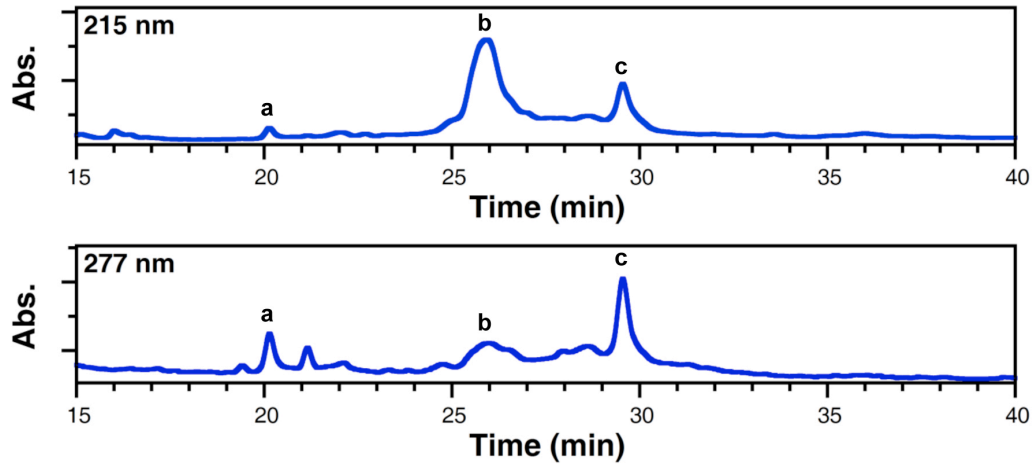

Figure S24. HPLC analysis of ligation of Ac-αS^{F}V′$_3$C$_9$F*$_{39}$. Peaks **a**, **b**, and **c**, correspond to hydrolyzed Ac-αS$_{1\text{-}8}$V′$_3$ thioester, αS$^{F}_{\Delta 1\text{-}8}$C$_9$F*$_{39}$, and ligation product Ac-αS^{F}V′$_3$C$_9$F*$_{39}$. Peaks earlier than **b** correspond to hydrolyzed peptide side products.

Mass Spectrometry of Ac-αS^{F}F′$_4$C$_9$F*$_{39}$.

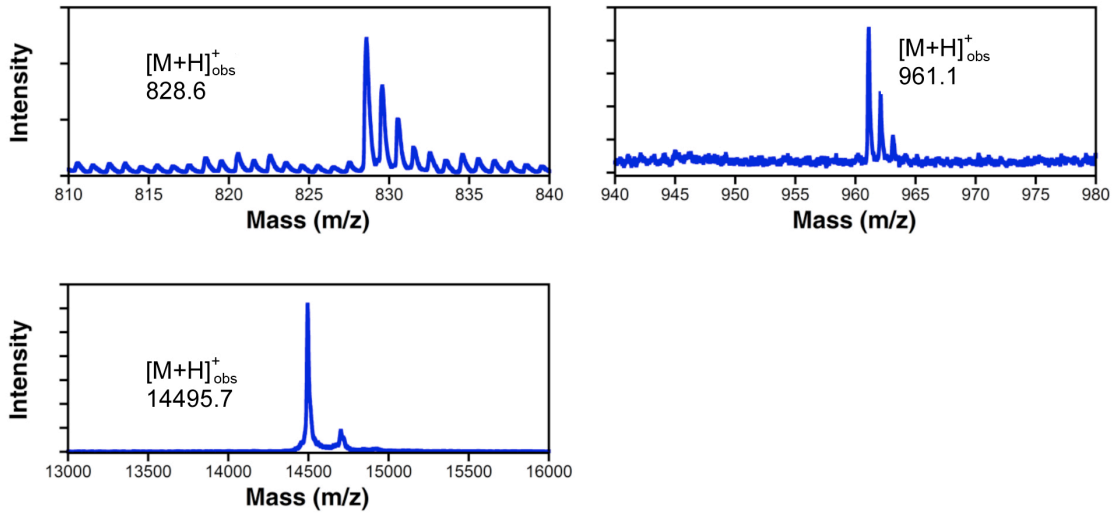

Figure S25. MALDI MS analysis of Ac-αS^{F}F′$_4$C$_9$F*$_{39}$ (bottom) and trypsin fragments containing thioamide (top left) or Cnf (top right). Calcd m/z of thioamide-containing trypsin fragment 1-8: 828.4. Calcd m/z of Cnf-containing trypsin fragment: 961.1 Calcd m/z of of Ac-αS^{F}F′$_4$C$_9$F*$_{39}$: 14494.7

UV Absorbance and Primary Fluorescence Spectra of Ac-αS^{F}F′$_4$C$_9$F*$_{39}$.

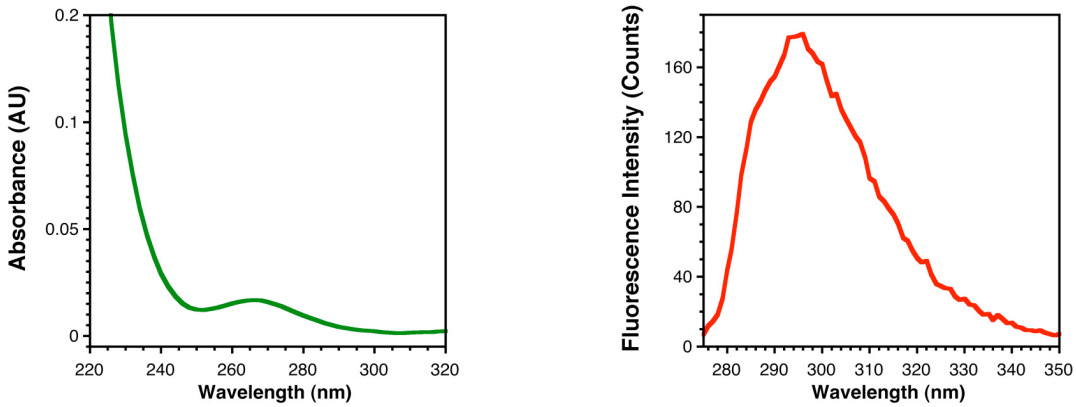

Figure S26. UV absorbance (left) and fluorescence spectrum (right) of Ac-αS^{F}F′$_4$C$_9$F*$_{39}$. 1 μM samples were prepared in Tris buffer (20 mM Tris, 100 mM NaCl, 1 mM BME, pH 7.5).

b c

Mass Spectrometry of Ac-αS^{F}V′$_3$C$_9$F*$_{39}$.

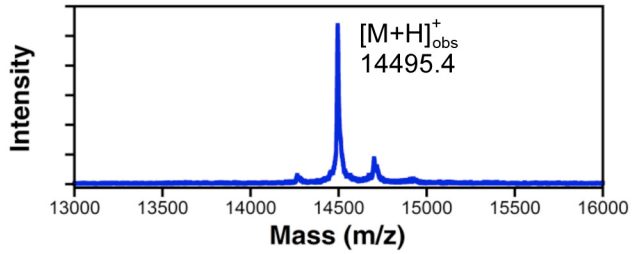

Figure S27. MALDI MS analysis of Ac-αS^{F}V′$_3$C$_9$F*$_{39}$. Calcd m/z of Ac-αS^{F}V′$_3$C$_9$F*$_{39}$:14494.7.

HPLC Analysis of αS^{F}F*$_{39}$ C$_{123}$A′$_{124}$.

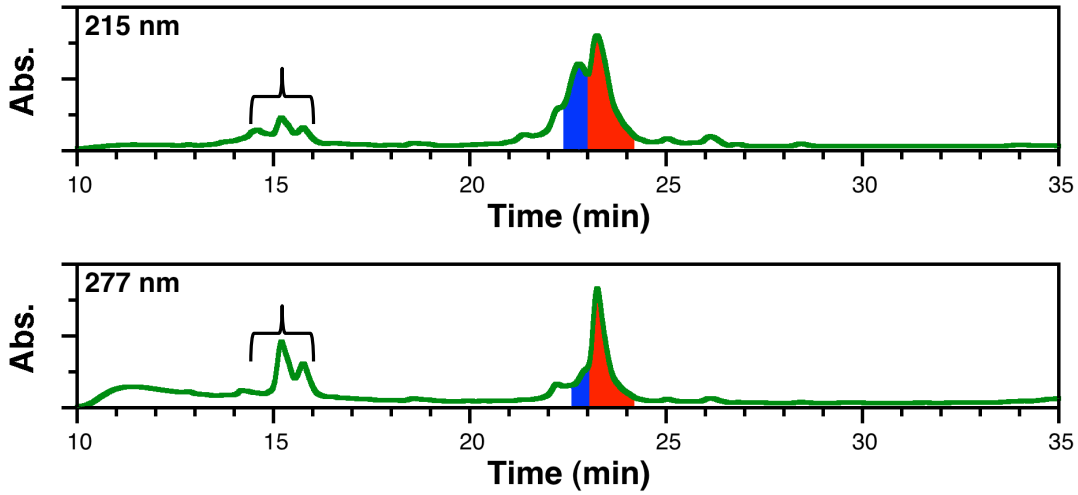

Figure S28. HPLC analysis of αS^{F}F*$_{39}$ C$_{123}$A′$_{124}$. Peaks under bracket **a** correspond to thioamide peptide and thioamide peptide side products. Unligated αS$_{1\text{-}122}$F*$_{39}$ (**b**) and ligated product αS^{F}F*$_{39}$C$_{123}$A'$_{124}$ (**c**) are represented by the blue and red shaded regions, respectively.

FPLC Analysis of αS^{F}F*$_{39}$C$_{123}$A′$_{124}$.

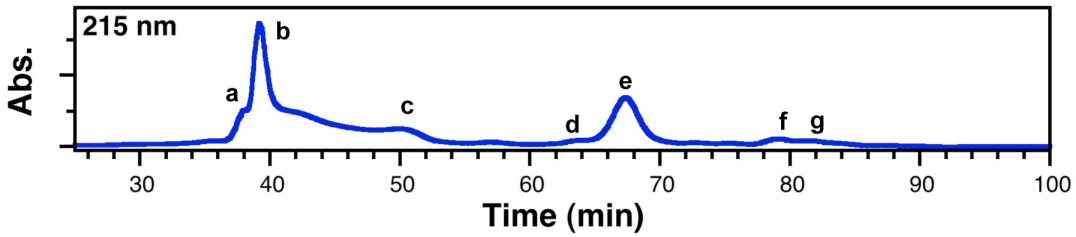

Figure S29. FPLC analysis of αS^{F}F*$_{39}$C$_{123}$A′$_{124}$. Peaks **a**, **b**, and **c** correspond to hydrolyzed αS$_{1\text{-}122}$F*$_{39}$SR (αS$_{1\text{-}122}$F*$_{39}$OH), TCEP, and protein impurities in the 8-9 kDa range. Peaks **d**, **e**, and **f**, and **g** correspond to thioamide peptide side products, αS^{F}F*$_{39}$C$_{123}$A'$_{124}$, thioamide peptide-ligated protein dimer, and thioamide peptide dimer.

MALDI MS Analysis of αS$^{F}_{1-122}$F*$_{39}$-SR Formation.

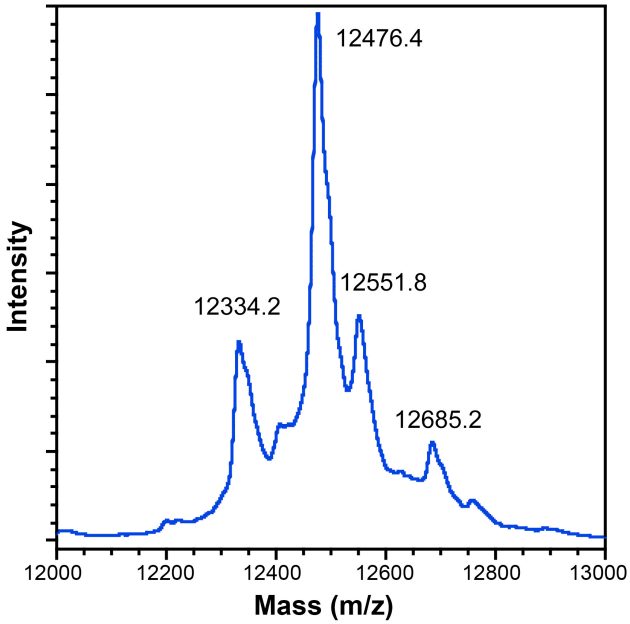

Figure S30. MALDI MS analysis of αS$^{F}_{1-122}$F*$_{39}$-Intein thiolysis reaction. Calcd m/z of αS$^{F}_{1-122}$F*$_{39}$-OH (M+H^{+}): 12350.0, Calcd m/z of αS$^{F}_{1-122}$F*$_{39}$-Suc (M+H^{+}): 12332.0, Obsvd = 12334.2 (structure below); Calcd m/z of αS$^{F}_{1-122}$F*$_{39}$-SR (M+H^{+}): 12475.2 Obsvd: 12476.4 (structure below). Succinimidyl (Suc) cyclizations are commonly observed for C-terminal Asn residues. See, for example InBase intein protein database (http://tools.neb.com/inbase/index.php).[13]

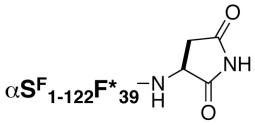

αS$^{F}_{1-122}$F*$_{39}$-Suc

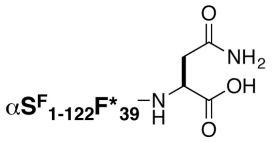

αS$^{F}_{1-122}$F*$_{39}$-OH

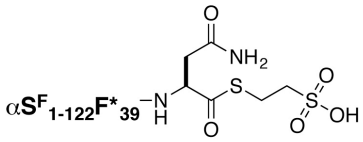

αS$^{F}_{1-122}$F*$_{39}$-SR

Absorbance Measurements of Thioacetamide in Trimethylamine Oxide. The absorbance of thioacetamide (approximately 35 μM) was measured in Tris buffer (20 mM Tris, 100 mM NaCl, 1 mM BME, pH 7.5) and in Tris buffer containing 4M trimethylamine oxide. This verified that TMAO did not alter the ability of the thioamide to participate in FRET.

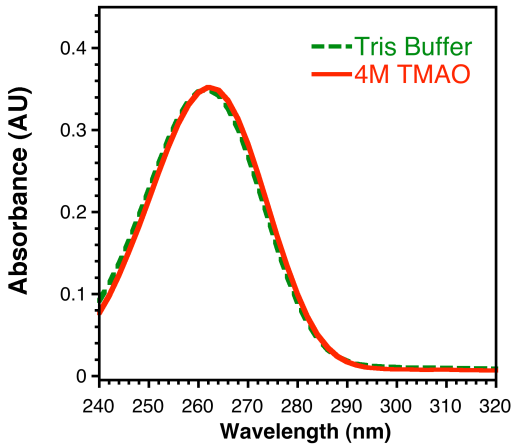

Figure S31. Thioacetamide absorbance in Tris buffer compared to thioacetamide absorbance in Tris buffer containing 4M TMAO.

Fluorescence Measurements of Cnf in Trimethylamine Oxide. The fluorescence of 1 μM Cnf amino acid was measured in 20 mM Tris, 100 mM NaCl, pH 7.5 containing 0, 1, 2, 3, or 4M TMAO. A decrease in fluorescence is observed at higher TMAO concentrations.

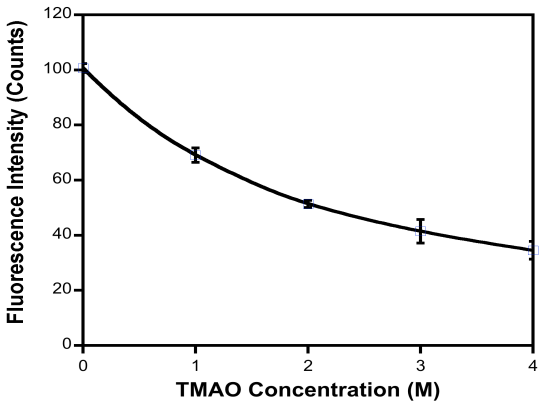

Figure S32. Fluorescence intensity of Cnf at 295 nm in increasing concentrations of TMAO upon excitation with 240 nm light.

Fluorescence Measurements of αS Mutants in Trimethylamine Oxide and Urea. Samples were prepared as described in the main text. The background fluorescence of each buffer was independently measured and subtracted from the protein fluorescence spectrum.

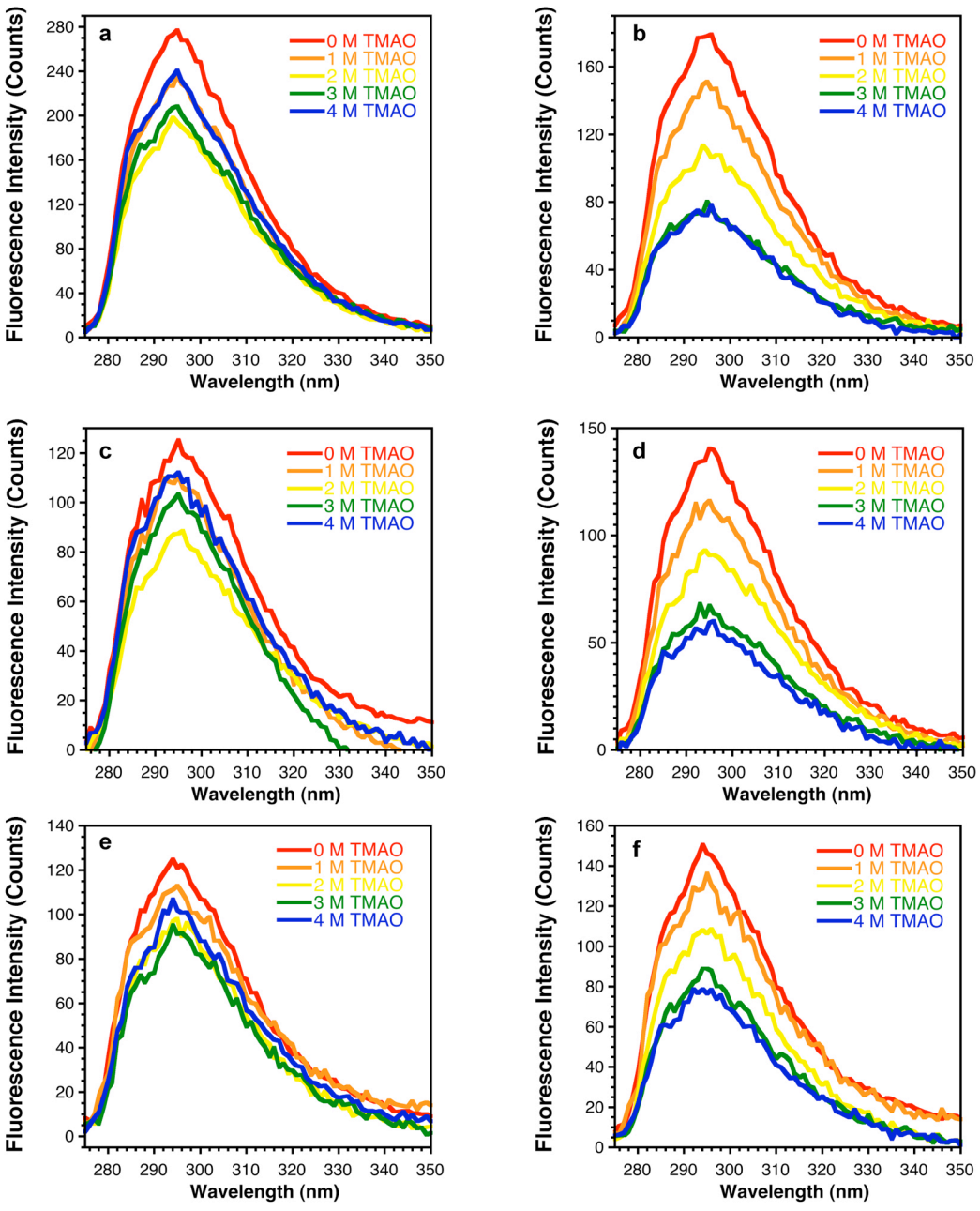

Figure S33. Fluorescence scans of oxoamide and thioamide-containing αS mutants in increasing concentrations of TMAO: $\alpha S^{F}C_{9}F^{*}_{39}$ (**a**), Ac-$\alpha S^{F}F'_{4}C_{9}F^{*}_{39}$ (**b**), $\alpha S^{F}C_{9}F^{*}_{94}$ (**c**), Ac-$\alpha S^{F}F'_{4}C_{9}F^{*}_{94}$ (**d**), $\alpha S^{F}F^{*}_{39}$ C_{123} (**e**), $\alpha S^{F}F^{*}_{39}$ $C_{123}A'_{124}$ (**f**).

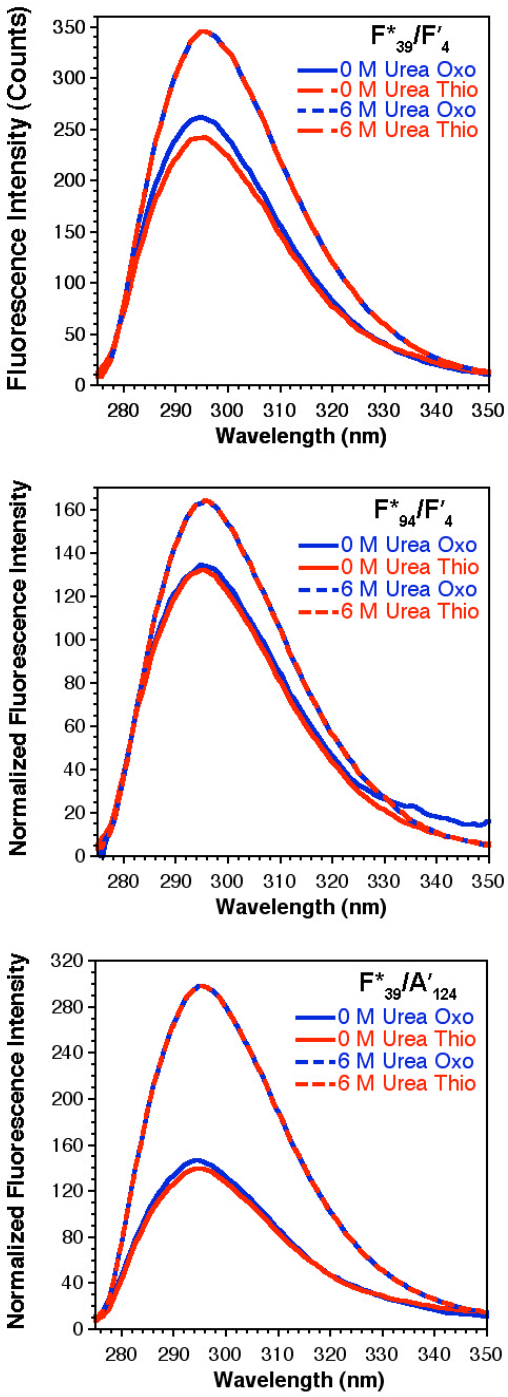

Figure S34. Normalized fluorescence scans of oxoamide and thioamide-containing αS mutants in 0 and 6 M Urea: Top: $\alpha S^{F}C_{9}F^{*}_{39}$ and Ac-$\alpha S^{F}F'_{4}C_{9}F^{*}_{39}$, Middle: $\alpha S^{F}C_{9}F^{*}_{94}$ and Ac-$\alpha S^{F}F'_{4}C_{9}F^{*}_{94}$, Bottom: $\alpha S^{F}F^{*}_{39}$ C_{123} and $\alpha S^{F}F^{*}_{39}$ $C_{123}A'_{124}$.

Experimental Förster Distance Calculations (αS). The Förster distance, R_0, was calculated using equations (S1), (S2), (S3), and (S4) as described above for CaM. Substituting $J = 7.0\times10^{12} \pm 2\times10^{11}$ $M^{-1}\bullet cm^{-1}\bullet nm^4$ into equation (S1), as well as 0.11 for the quantum yield of Cnf, 1.33 for the index of refraction of water, and 2/3 for κ^2 gives R_0 = 15.6 Å for $\alpha S^F C_9 F^*_{39}$ constructs in 0 M TMAO. For $\alpha S^F C_9 F^*_{94}$ constructs, we use 0.049 as a quantum yield for Cnf, and calculate R_0 = 13.6 Å. For $\alpha S^F F^*_{39} C_{123}$ constructs, we use 0.045 as a quantum yield for Cnf, and calculate R_0 = 13.5 Å. In all cases data in 6 M urea were used to normalize oxo-and thio-fluorescence data to ensure that small deviations in concentration did not alter data interpretation. Quantum yields for each mutant in different concentrations of TMAO were determined by comparing the fluorescence output of the mutant relative to the fluorescence of that mutant in 0 M TMAO using identical concentrations and fluorometer settings. Comparison of $\alpha S^F C_9 F^*_{39}$ fluorescence to free Cnf showed that no substantial quenching occurred in this mutant in the absence of the thioamide (data not shown). As for CaM, these values of R_0 were then used in determining experimental chromophore separations (R_{FRET}) for each set of Cnf/thioamide probe locations according to equation (S5) where E_Q is defined by equation (S6) as described in the main text. These calculations are summarized in Table S7.

Table S8. R_{FRET} Determination in α-Synuclein Refolding Assay[a]

	$\alpha S^{F}F'_{4}C_{9}F^{*}_{39}$		$\alpha S^{F}F'_{4}C_{9}F^{*}_{94}$		$\alpha S^{F}F^{*}_{39}C_{123}A'_{124}$	
[TMAO]	E_Q	SE	E_Q	SE	E_Q	SE
0	0.13	0.02	-0.02	0.02	0.03	0.06
1	0.14	0.01	0.07	0.03	0.02	0.02
2	0.24	0.02	0.08	0.03	0.07	0.03
3	0.48	0.03	0.31	0.03	0.24	0.02
4	0.59	0.03	0.59	0.07	0.40	0.05
[TMAO]	R_{FRET}	SE	R_{FRET}	SE	R_{FRET}	SE
0	21.3	0.7				
1	20.5	0.4	20.8	1.7	24.5	4.2
2	17.9	0.4	19.2	1.5	20.1	1.4
3	15.2	0.3	14.8	0.4	15.8	0.3
4	14.4	0.3	12.6	0.6	14.1	0.5
[TMAO]	F_{Oxo}	R_0	F_{Oxo}	R_0	F_{Oxo}	R_0
0	282.2	15.6	125.3	13.6	115.9	13.5
1	243.9	15.2	110.8	13.4	106.2	13.3
2	204.7	14.8	87.4	12.8	90.2	12.9
3	220.8	15.0	93.4	13.0	93.2	13.0
4	257.5	15.4	112.3	13.4	102.0	13.2

[a] Parameters calculated as described in Supporting Information text. All distances in Å.

References

(1) Demick, K. A., Boston College, 2009.
(2) Shalaby, M. A.; Grote, C. W.; Rapoport, H. *J. Org. Chem.* **1996**, *61*, 9045-9048.
(3) Stevens-Truss, R.; Marletta, M. A. *Biochemistry* **1995**, *34*, 15638-15645.
(4) Goldberg, J. M.; Wissner, R. F.; Klein, A. M.; Petersson, E. J. *Chem. Commun.* **2012**, *48*, 1550-1552.
(5) Forster, T. *Disc. Faraday Soc.* **1959**, 7-17.
(6) Van Der Meer, B. W.; Coker III, G.; Chen, S.-Y. S. *Resonance Energy Transfer*; VCH Publishers, Inc.: New York, NY U.S.A., 1994.
(7) Goldberg, J. M.; Batjargal, S.; Petersson, E. J. *J. Am. Chem. Soc.* **2010**, *132*, 14718-14720.
(8) Tucker, M. J.; Oyola, R.; Gai, F. *Biopolymers* **2006**, *83*, 571-576.
(9) Contessa, G. M.; Orsale, M.; Melino, S.; Torre, V.; Paci, M.; Desideri, A.; Cicero, D. O. *J. Biomol. NMR* **2005**, *31*, 185-199.
(10) Batjargal, S.; Wang, Y. J.; Goldberg, J. M.; Wissner, R. F.; Petersson, E. J. *J. Am. Chem. Soc.* **2012**, *134*, 9172-9182.
(11) Peeler, J. C.; Mehl, R. A. In *Unnatural Amino Acids: Methods and Protocols*; Pollegioni, L., Servi, S., Eds. 2012; Vol. 794, p 125-134.
(12) Sambrook, S.; Russell, D.W. Molecular Cloning, 3rd ed.; Cold Spring Harbor Laboratory Press: Cold Spring Harbor, New York, 2001.
(13) Perler, F. B. *Nucleic Acids Res.* **2002**, *30*, 383-384.